2022 NDIA MICHIGAN CHAPTER
GROUND VEHICLE SYSTEMS ENGINEERING
AND TECHNOLOGY SYMPOSIUM
<ADVANCED MATERIALS & MANUFACTURING> TECHNICAL SESSION
AUGUST 16-18, 2022 - NOVI, MICHIGAN

SUPERIOR BALLISTIC AND BLAST RESISTANCE IN ATI TITAN 27™ ALLOY WITH A NOVEL DEFORMATION MECHANISM

John Foltz[1], Luis Ruiz-Aparicio[1], David Berry[1], Rick Porter[1]
[1] ATI. 500 Green Street, Washington PA 15301.

ABSTRACT

α-β titanium alloys are used in armor plate applications due to their capability to defend against ballistic threats while having a 40% lower density than steel. ATI 425® was developed as a cold-deformable alternative to Ti-6Al-4V with similar ballistic properties and improved blast performance owing to the alloy's higher damage tolerance. ATI Titan 27™ is an evolutionary step forward on ATI 425® Alloy, and is being developed as a higher-performance titanium armor alloy owing to its greater than 10% improvement in strength with similar ductility and formability. Recent work has demonstrated a novel deformation mechanism that explains the improved cold deformation observed in both alloys over Ti-6Al-4V. This mechanism, a twinning of α-phase coinciding with slip in the β-phase, is unique among high-strength titanium alloys. Moreover, twinning is well known to be suppressed with high oxygen content, and ATI Titan 27™ Alloy has one of the highest oxygen targets across high-strength α-β titanium alloys. Mechanical properties and ballistic results of ATI Titan 27™ Alloy will be covered, as well as results from an in-situ microscopy deformation study demonstrating the slip-twinning mechanism. Typical results for ATI Titan 27™ will be compared to the ATI Ti-6Al-4V alloy, of which ATI has manufactured more than 16 million pounds for armor plate.

Citation: Foltz, Ruiz-Aparicio, Berry, Porter, "Superior Ballistic and Blast Resistance in ATI Titan 27™ Alloy with a Novel Deformation Mechanism," In *Proceedings of the Ground Vehicle Systems Engineering and Technology Symposium* (GVSETS), NDIA, Novi, MI, Aug. 16-18, 2022.

1. INTRODUCTION

ATI supplies titanium plate, sheet and other product forms to the Defense industry for applications requiring high specific strength. The most common alloy of titanium for these applications is Ti-6Al-4V, and it demonstrates adequate ballistic and blast resistance when used in conjunction with other materials for personnel and vehicle armor.

Vehicle fuel efficiency and freight transportability is strongly affected by weight [1], and this is an area where titanium alloys offer performance gains over steel alloys. Applique armor systems can be light-weighted by approximately 30% when moving from steel to titanium. To further improve upon that, ATI has developed in recent years several new titanium alloys with improved properties over Ti-6Al-4V. ATI 425® Alloy (*herein referred to as Ti-425*) has increased cold deformation capability over Ti-6Al-4V, and has been used as an armor alloy since approximately 2008. ATI Titan 27™ Alloy (*herein referred to as Ti-27*) is a newer alloy and has higher strength while maintaining the cold deformation capability of Ti-425. Given the improved properties of ATI Titan 27™, on-range performance of the alloy has been measured from hot rolled plate.

2. Materials & Processing

Two alloys were compared to commercial Ti-6Al-4V military plate. These two alloys as described herein included Ti-27 and Ti-425.

One heat of Ti-27 plate was manufactured for the study, made via electron-beam cold-wall hearth

melting. The heat was open die press-forged to slab, and then converted to plate via hot rolling on small production-scale equipment. Hot rolling was conducted in the α + β phase field, and the plate was reduced to 30mm thickness. The material was unidirectionally rolled due to size-based processing limitations, resulting in increased texture and elongated primary α grains in the rolling direction. Comparatively, production material is typically cross-rolled to balance properties in orthogonal directions.

Ti-425 and ATI Ti 6-4™ Alloy (*herein referred to as Ti-64*) for this study was produced by electron-beam cold hearth melting, and bi-directionally rolled to plate in the alloy's α + β phase field. Both are commercially available products meeting the requirements of MIL-DTL-46077G Class 4 and Class 2titanium armor, respectively [2].

Ballistic testing of the three materials was completed by NTS Chesapeake Testing and Aberdeen Test Center. The projectile used was a 20mm fragment simulating projectile (FSP), tested to MIL-DTL-46077G. Obliquity was 0° in all testing.

Tensile testing of the material was completed using in-house NADCAP approved testing laboratories, using procedures compliant to ASTM E-8 [3]. Similarly, chemistry testing was completed using in-house test facilities that employ spark-plasma OES, mass spectrometry, and combustion to measure metals and impurities such as oxygen and hydrogen.

Microstructures were examined using scanning electron microscopy. Sample preparation for this inspection followed conventional sanding with silicon carbide and polishing with alumina and silica abrasives. A combination of backscattered electron imaging and electron backscattered electron diffraction (EBSD) mapping to understand the micromechanics of Ti-425 and Ti-27. This was conducted at the Massachusetts Institute of Technology using a scanning electron microscope equipped with *in-situ* tensile testing capability, which was utilized to understand the deformation of prepolished samples.

3. Results

Ballistic data from many thicknesses of ATI 6-4™ Alloy and Ti-425 were compared with the Ti-27, and were done so by the degree above the V-50 requirements of Class IV titanium armor for their given thickness as shown in (1):

$$\Delta V50 = V50_{Actual} - V50_{required} \quad (1)$$

The results of this comparison are shown in Table 1. ATI Titan 27™ was heat treated to two different mill annealing temperatures as indicated in the table, and experienced similar results between the two conditions. Additionally, the ΔV50 of ATI Titan 27™ was above the average for both ATI 6-4™ and Ti-425 in this limited testing.

Table 1: Experimental V50 results. Ti-425 and Ti-64 data represents historical production data of over 100 heats each.

Alloy	Thickness, mm	ΔV50
AVG. Ti-425 [4]	19-31	115
AVG. Ti-64 [4]	19-33	146
Ti-27 HT 1	30	163
Ti-27 HT 2	30	160

Mechanical properties for the alloys are shown in Table 2 for Ti-425 and Ti-27, in comparison to Ti-6Al-4V specification minimums in AMS 4911 and MIL-DTL 40677Class 2/4G. Chemistry results for Ti-27 are shown in Table 3.

Scanning electron microscopy (SEM) of the Ti-27 is shown in Figure 1. The microstructure consists of equiaxed α grains, α laths formed from transformed β, and some residual elongated α phase

that did not fully dynamically recrystallize during processing. This microstructure is similar to Ti-425 and Ti-64 in armor plate products.

Table 2: Tensile properties of armor plate in comparison to Ti-6Al-4V and Ti-425.

Alloy	Property	Long.	Trans.
Ti-27	TYS	132	173
	UTS	144	180
	%EL	11	13
Ti-6Al-4V [1]	TYS	137	137
	UTS	145	145
	%EL	16	16
Ti-425 [1]	TYS	129	149
	UTS	141	157
	%EL	15	13

Table 3: Chemistry results of ATI Titan 27™.

	Al	V	Sn	Co	Fe	O
Ingot Top	4.4	5.26	3.56	1.21	0.127	0.22
Ingot Bot	3.99	4.38	2.79	0.96	0.123	0.178

Backscattered electron images were analyzed using MIPAR to semi-quantitatively assess the volume fraction of transformed β in the alloys. Ti-27 armor plate contains 83 area fraction of α phase, which is the darker color in Figure 1. In comparison, Ti-425 contains approximately 85 area fraction α-phase, and Ti-64 has 90 percent area fraction in mill annealed conditions.

4. Discussion

One differentiation between Ti-425 and Ti-6Al-4V is its unique ability to twin in the α phase during tensile testing. Prior work in Ti-6Al-4V has shown that at ballistic strain rates twinning can be activated, giving rise to additional damage mechanisms [5]. To further understand this deformation mode, and determine if it is also active in Ti-27, given its superior ballistic protection, an in situ microscopy study during tensile testing was conducted. The specific details of the preparation and testing are noted in a prior publication [6, 7]. **Error! Reference source not found.** shows the microstructure of Ti-425 during this tensile testing, with the stress applied and strain measured via digital image correlation noted. Throughout the testing, images were collected and

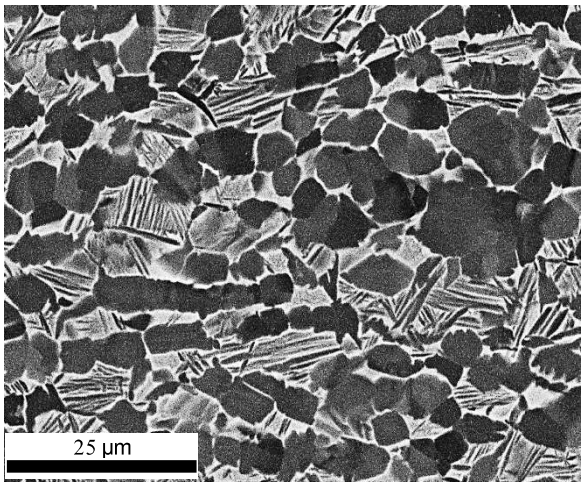

Figure 1: Backscattered electron image of ATI Titan 27™ Alloy in plate form for ballistic testing.

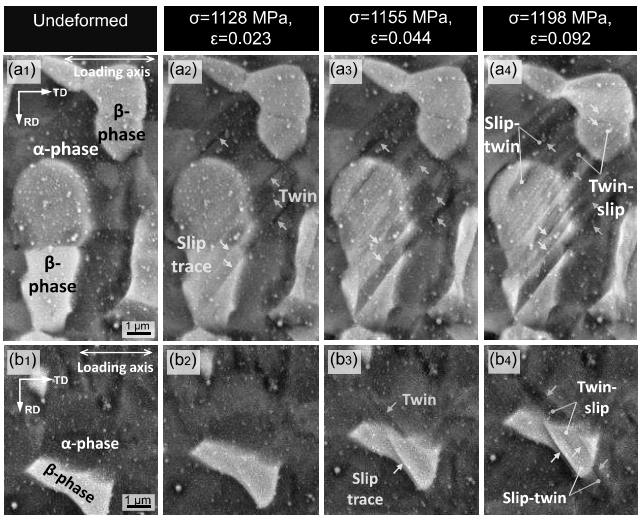

Figure 2: Micro DIC results while tensile testing ATI 425® Alloy [6].

afterwards the material was scanned using electron backscattered diffraction (EBSD). Slip-trace analysis was performed from the EBSD maps and SEM images to identify twinning from slip events. Unlike in other studies on Ti-6Al-4V [8], the Ti-

425 shown in **Error! Reference source not found.** appears to have closely-spaced shear planes, and notably many instances of twinning within the α phase. These twins in some cases, a1 through a4, initiate slip in the β phase. In other cases, b1 through b4, they appear to initiate from slip in the β phase.

The appearance of twinning in Ti-425 significantly reduces the amount of strain localization at α-β interfaces. In panel a1 of Figure 3, it is observed that strain can accumulate on the β side of the α-β interface when no slip or twinning has yet to activate in α phase. Panel a2 shows an example where less strain intensity builds in the α phase when the adjacent β phase has yet to form a shear band. Finally, panel a3 shows an example of where twinning within the α phase has accommodated and reduced the strain intensity at two β-α interfaces, resulting in a very delocalized strain field. This reduction of strain intensity is achieved through the similar orientation of the shear bands in the β phase and the twins in the α phase. Figure 4 graphically shows the reduction in strain localization experimentally measured from many of these EBSD studies in Ti-425. In grains that do not have twinning, and only have shear in either the α or β phases, intense strain localization follows the purple and black lines respectively. The activation of twinning in the α phase either prior to, or after the β phase shears reduces the local strain field by 3x-5x.

Literature indicates that more highly alloys titanium, specifically containing higher amounts of aluminum and or oxygen, tend to have reduced capability to twin the α phase [1, 9]; one example of this being Ti-6Al-4V. Hexagonal materials, in comparison to cubic materials, have far fewer independent deformation modes, including [1]:

- Two basal (0002) a-type slip system
- Two prism $\{10\bar{1}0\}$ a-type slip systems
- Four pyramidal $\{10\bar{1}1\}$ a-type slip systems
- Five pyramidal $\{11\bar{2}2\}$ c+a type slip systems

In comparison to these thirteen independent slip systems, face-centered cubic materials, such as stainless steels, have 24 independent slip systems, and body centered cubic materials such as low-carbon steel have 72 independent slip systems, all of which activate with relative ease. It should be noted that the five c+a type slip systems in titanium have approximately 2.5x the activation energy as the prism slip systems, which significantly decrease the material's ability to activate these modes of deformation [1].

Similar in situ tensile deformation studies to **Error! Reference source not found.** have been performed in Ti-27. In Figure 5, Ti-27 also demonstrates the ability to twin in the α phase, with low degrees of misorientation to slip in the β phase like Ti-425. This could explain the high degree of ductility and ballistic resistance observed in the alloy given the strength of the material being similar to both Ti-425 and Ti-64 in this study.

In both Ti-425 and Ti-27, tensile twinning has been observed. The addition of this $\{10\bar{1}2\}$ tensile twinning system adds five additional deformation modes; an increase of more than 30% independent modes of deformation. Given that in fracture mechanics of hexagonal materials shear localization gives rise to crack initiation sites which lead to fracture [10], the delocalization of strain

fields by twinning creates a unique mechanism in Ti-425 to delay fracture in comparison to Ti-64.

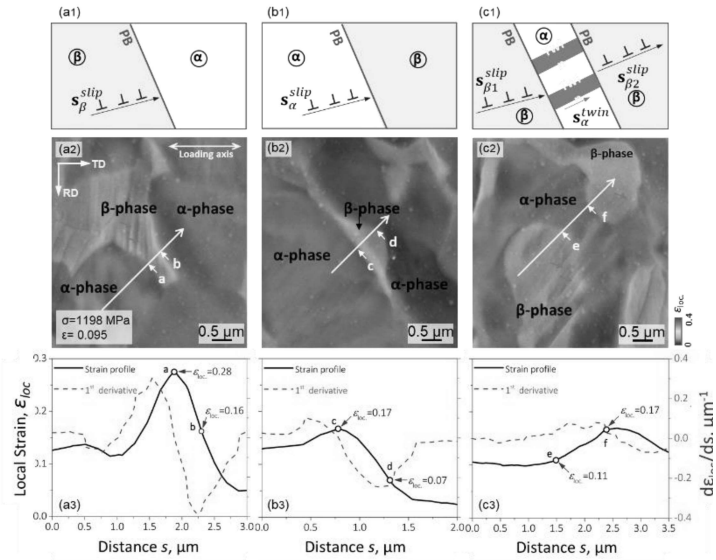

Figure 3: Microstrain accumulation in Ti-425 during in-situ tensile testing, measured using EBSD and digital image correlation. [12]

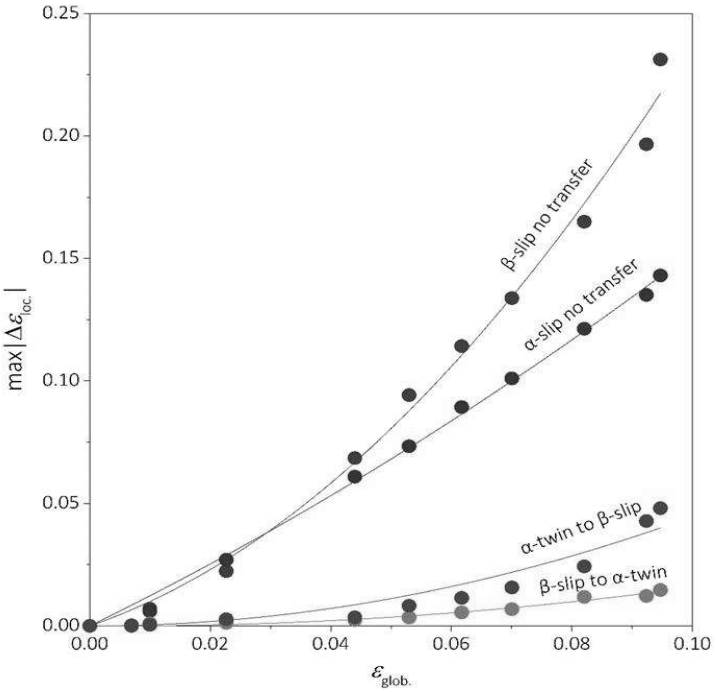

Figure 4: Effect of strain localization in Ti-425 at α-β interfaces based on specific deformation mechanisms active. [12]

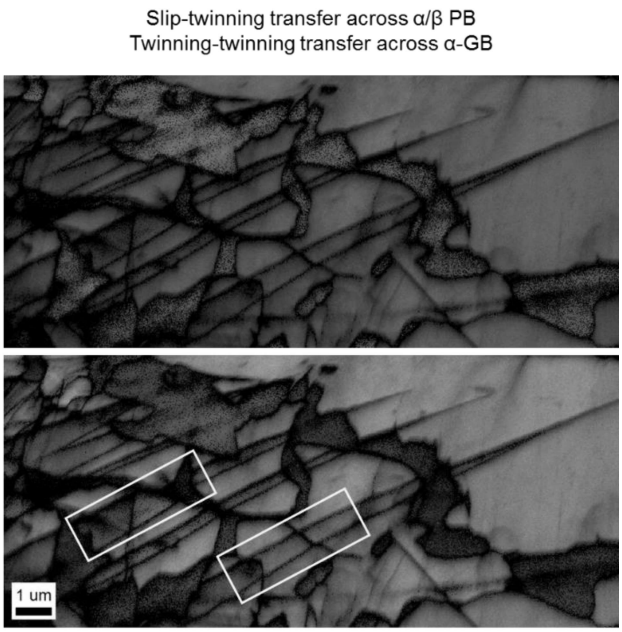

Figure 5: (Top) EBSD-derived phase map showing β phase in yellow and α phase in purple. (Bottom) EBSD map of Ti-27 showing twinning within α grains.

5. Conclusions

The V50 ballistic protection of Ti-27 and Ti-425 was compared with Ti-64 Alloy using 20mm FSP threats. Preliminary results indicate that Ti-27 has superior ballistic protection to both Ti-64 and Ti-425 alloys. In situ deformation studies using a combination of EBSD, and digital image correlation on secondary electron images indicate Ti-27 and Ti-425 are both capable of deforming in the α phase via tensile twinning in addition to the traditional slip systems observed in Ti-6Al-4V. This is one reason for the high degree of damage tolerance by ballistic threats observed in both alloys.

6. REFERENCES

[1] G. Lütjering and J.C. Williams, "Titanium" Springer-Verlag, Berlin, 2007.

[2] "Armor Plate, Titanium Alloy, Weldable" ARL Weapons and Materials Research Directorate MIL-DTL-46077F, Specifications and Standards Office.

[3] "Standard Test Methods for Tension Testing of Metallic Materials" ASTM E8/E8M-21, in Annual Book of ASTM Standards, vol. 3.01. DOI: 10.1520/E0008_E0008M-21.

[4] Unpublished, internal data. 2022.

[5] Lainé et al., "Very high strain rate deformation twinning behaviour of Ti-6Al-4V", Materialia, Vol 12, Aug 2020, https://doi.org/10.1016/j.mtla.2020.100762 .

[6] Wei et al. "Slip-twinning interdependent activation across phase boundaries: An *in-situ* investigation of a Ti-Al-V-Fe (α+β) alloy", Acta Materialia, Vol 206, Mar 2021, https://doi.org/10.1016/j.actamat.2020.116520 .

[7] Wei et al. "In-situ investigation of plasticity in a Ti-Al-V-Fe (α+β) alloy: Slip mechanisms, strain localization, and partitioning", International Journal of Plasticity, Vol 148, Jan 2022, https://doi.org/10.1016/j.ijplas.2021.103131 .

[8] JW Foltz and SM Schlegel, "Deformation Studies of Titanium Wire for Fastening Systems Performance", Proceedings of the 13th World Conference on Titanium, John Wiley & Sons, Inc, Hoboken NJ, May 2016.

[9] Laine, S. J. (2017). The Role of Twinning in the Plastic Deformation of Alpha Phase Titanium (Doctoral thesis). https://doi.org/10.17863/CAM.13395

[10] George Dieter, "Mechanical Metallurgy", McGraw-Hill, New York, 1961, P. 247.

[11] Melvin Kanninen and Carl Popelar, "Advanced Fracture Mechanics", Oxford Press, New York, 1985, P. 272

[12] Foltz et al., "Understanding Room Temperature Deformation of High-Strength Titanium Alloys", Microscopy and Microanalysis, Vol 27 S1, Aug 2021, p28-29, https://doi.org/10.1017/S1431927621000696 .